

Solubility and Dissolution Thermodynamics of Molecular Perovskite Energetic Material

YUAN Ming-yu¹, LIU Qiang-qiang¹, SHANG Yu², ZHOU Wei¹, ZOU Li¹, GAO Hai-xiang³, LIU Ying-le¹

(1. School of Chemistry and Environmental Engineering, Sichuan University of Science & Engineering, Zigong 643000, China; 2. Xi'an Modern Chemistry Research Institute, Xi'an 7100651, China; 3. Department of Applied Chemistry, China Agricultural University, Beijing 100193, China)

Abstract: Solubility is an important parameter for the crystallization of molecular perovskite energetic materials ($\text{H}_6\text{N}_2\text{H}_{14}$)[$\text{NH}_4(\text{ClO}_4)_3$](DAP-4). In this work, the dissolution behaviors of DAP-4 at different temperatures (288–323 K) and in different solvents (ethanol, ethyl acetate, formic acid, deionized water, acetone, cyclohexane, methanol, acetonitrile, *n*-propanol) were studied by the gravimetric method. The dissolution models were established by the Apelblat equation and the λh equation, respectively. Meanwhile, the dissolution thermodynamic parameters (ΔH_d , ΔS_d , ΔG_d) were obtained by Van't Hoff equation based on the thermodynamic principle of solid-liquid equilibrium. Results show that the solubility of DAP-4 is the largest in water and the smallest in ethyl acetate, which are increased with the increasing of temperature in different solvents. The fitting result of dissolution model from the Apelblat equation is better than that of the λh equation. Positive values of ΔH_d , ΔS_d , and ΔG_d indicate that the dissolving process of DAP-4 are non-spontaneous endothermic.

Key words: solubility; gravimetric method; molecular perovskite energetic material; dissolution thermodynamics parameters

CLC number: TJ55; O62

Document code: A

DOI: 10.11943/CJEM2022284

0 Introduction

Energetic compounds play an important role in military and civil fields^[1-3]. In recent decades, the research of energetic materials has progressed rapidly, and various new energetic materials have emerged, such as high nitrogen-containing heterocyclic compounds^[4-6], cage molecules with more energetic

groups ($-\text{NO}_2$, $-\text{NNO}_2$, $-\text{N}_3$, $-\text{C}(\text{NO}_2)_3$, etc.)^[7], energetic salts^[8-10], energetic cocrystals^[11-14], energetic metal complexes^[15-17] and molecular perovskite energetic material, etc.^[18-22]. Among of them, the molecular perovskite energetic material presents the advantages of excellent comprehensive performance, simple synthetic process, and low cost, which enables it to have good application prospects and has attracted widespread attention^[23-25]. In particular, the first metal-free member, (H_2dabco)(NH_4)(ClO_4)₃ (DAP-4, $\text{H}_2\text{dabco}_2^+=1,4$ -diazabicyclo [2.2.2] octane-1, 4-dium) exhibits great application potential as heat-resistant explosive^[21].

It is well known that the dissolution behavior of energetic materials under different temperatures and solvents can greatly affect the purity, morphology, and particle size of the product^[26], and then affect the safety performance such as sensitivity and thermal stability. Therefore, the study of dissolution behavior is of great significance to their purification,

Received Date: 2022-11-23; **Revised Date:** 2023-01-17

Published Online: 2023-06-01

Project Supported: Supported by the National Natural Science Foundation of China (No. 22005206, 22075318), Science and Technology Department of Sichuan Province (No. 2022NSFSC1209, 2022NSFSC0219), and Undergraduate Training Programs for Innovation and Entrepreneurship (No. cx2022046)

Biography: YUAN Ming-yu (1997-), female, postgraduate, doing in the modification of energetic materials and thermochemical research. e-mail: 291936139@qq.com

Corresponding Author: LIU Qiang-qiang (1987-), male, lecturer, doing in the design and theoretical simulation of nitrogen-rich energetic compounds. e-mail: liuqq87@163.com

LIU Ying-le (1986-), male, professor, doing in the design and synthesis of fluorine-rich nitrogen-rich energetic materials. e-mail: liuyingleyou@163.com

引用本文: 袁明羽, 刘强强, 尚宇, 等. 分子钙钛矿含能材料($\text{C}_6\text{N}_2\text{H}_{14}$)(NH_4)(ClO_4)₃(DAP-4)在288~323 K下的各种溶剂中的溶解度[J]. 含能材料, 2023, 31(11): 1116-1123.

YUAN Ming-yu, LIU Qiang-qiang, SHANG Yu, et al. Solubility and Dissolution Thermodynamics of Molecular Perovskite Energetic Material[J]. *Chinese Journal of Energetic Materials (Hanneng Cailiao)*, 2023, 31(11):1116-1123.

Chinese Journal of Energetic Materials, Vol.31, No.11, 2023 (1116-1123)

含能材料

www.energetic-materials.org.cn

separation, and modification. However, most research on DAP-4 is focused on its synthesis^[19], combustion performance, hygroscopicity and safety, as well as application in the formula of heat-resistant explosive^[27-30], and there is no report on its dissolution behavior.

In this work, the solubilities of DAP-4 in ethyl acetate, anhydrous ethanol, acetone, formic acid, cyclohexane, methanol, acetonitrile, *n*-propanol, and deionized water in the range of 288–323 K were systematic studied by the gravimetric method. Linear fitting was carried out based on the Apleblat equation^[31-33] and λh equation^[34-35], and the influence of temperature on the solubility variation was analyzed and discussed. The thermodynamic behavior of DAP-4 was analyzed with an ideal solution model, which may provide a reference for selecting suitable solvent in subsequent crystallization, purification, and surface modification of DAP-4.

1 Experimental section

1.1 Materials and Experimental apparatus

The powder samples of DAP-4 were obtained according to the previous work^[19]. Its phase purity was characterized by X-ray powder diffraction pattern. Ethyl acetate, absolute ethanol, acetone, methanol, acetonitrile, cyclohexane, *n*-propanol and formic acid are all analytical reagent, and deionized water is prepared by our laboratory.

Low temperature constant temperature bath: DLSB-5L/40 (± 0.5 K), Gongyi Yuhua Instrument Co., Ltd; Thermostatic water bath: HH-8 (± 0.5 K), Shanghai Lichen Instrument Technology Co., Ltd; Analytical balance: ME104 (± 0.1 mg), Mettler Toledo Technology (China) Co., Ltd; Pipettor: Shanghai Lichen Instrument Technology Co., Ltd.

1.2 Experimental

In the constant temperature oil bath of 288, 293, 298, 303, 308, 313, 318 K and 323 K, the excess DAP-4 were added into a certain volume of single solvent (such as deionized water, methanol, acetonitrile and formic acid: 50 mL; ethyl acetate,

cyclohexane, and *n*-propanol: 200 mL; absolute ethanol and acetone: 100 mL), and then stirred for 24 h to obtain saturated solution.

When the dissolution of DAP-4 reaches the equilibrium, a certain volume of saturated solvent was injected in the weighing bottle as m_0 with a syringe, sealed and weighed, and its mass was denoted as m_1 . The weighing bottle was then placed into a drying box and dried to a constant weight, at which time the mass was denoted as m_2 . All the experiments were repeated for three times. Therefore, the mole fraction solubility x_i of the solute can be calculated by the following Eq.(1):

$$x_i = \frac{\frac{m_2 - m_0}{M_1}}{\frac{m_2 - m_0}{M_1} + \frac{m_1 - m_2}{M_2}} \quad (1)$$

where M_1 is the molecular weights of solute, $\text{g}\cdot\text{mol}^{-1}$; M_2 is the molecular weights of solvent, $\text{g}\cdot\text{mol}^{-1}$.

The Class A uncertainty is calculated by Eq.(2)^[31]:

$$u_A = \sqrt{\frac{\sum_{i=1}^n (x_i - x_{cal})^2}{n(n-1)}} \quad (2)$$

where x_i is mole fraction solubility; x_{cal} is calculated mole fraction solubility; n is the number of data points for experimental measurement of solubility coefficient.

2 Results and Discussion

2.1 Solubility

Fig. 1 shows the characteristic XRD patterns of raw DAP-4 and the solids equilibrated with different pure solvents. As indicated, the positions of characteristic peaks (2θ) of the equilibrium solid phase are quite close to those of the raw DAP-4. As a result, no solvation or polymorph transformation phenomenon took place before and after experiments.

The solubility of DAP-4 in ethyl acetate, absolute ethanol, acetone, formic acid, deionized water, cyclohexane, methanol, acetonitrile, and *n*-propanol were studied by the gravimetric method in the range of 288–323 K. The results are shown in

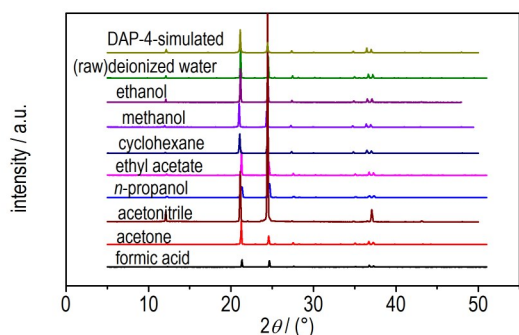


Fig. 1 XRD curves of raw DAP-4 and equilibrated solids in different solvents

Table S1 and Fig.2. As well known, DAP-4 is polar compound. According to the theory of similar dissolve mutually, it has the largest solubility in water, and the smallest in ethyl acetate. From the solubility in Fig.2a and 2b, it can be seen that the dissolution order of DAP-4 in each pure solvent is roughly as follows: ethyl acetate<cyclohexane<*n*-propanol<absolute ethanol<acetone<methanol<acetonitrile<formic acid<deionized water, which is consistent with the theoretical results. The solubility of DAP-4 in deionized water and formic acid is significantly better

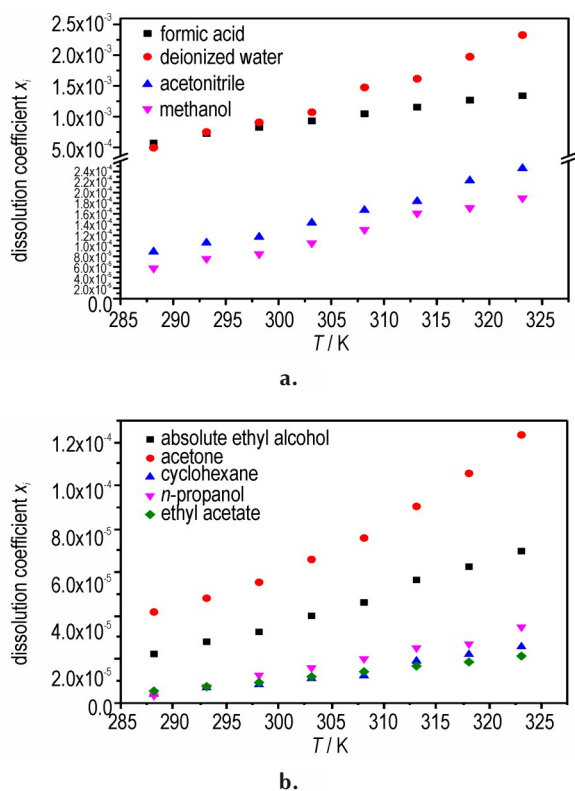


Fig. 2 Solubilities of DAP-4 in different solvents ((a) and (b) are the x_i - T diagrams, respectively)

than the other solvents. Except for deionized water and formic acid, some solubility curves of DAP-4 are very close or have a certain degree of crossover, which might be caused by the change of solute activity coefficients. In addition, the experimental results are not completely consistent with the polarity order of the solvents, and the degree of solubility change with temperature is also different in various solvents. The solubility of DAP-4 in deionized water has the strongest dependence on temperature, while the solubility in ethyl acetate has the worst dependence on temperature. It shows that the complex interactions between DAP-4 and the tested solvents can be affected not only by polarity of the solvents, but also by other factors, such as molecular size, spatial conformation, and the ability to form hydrogen bonds. According to the above experimental results, deionized water and formic acid with better solubility were selected as co-solvents, and ethyl acetate and *n*-propanol with poor solubility were selected as the anti-solvent during purification and recrystallization of DAP-4.

2.2 Dissolution model of DAP-4

The thermodynamic model for solid-liquid equilibrium is helpful to predict the solubility of energetic materials, which enables purification and recrystallization for high quality crystal. In this paper, the modified Apelblat model and the λh model were used to correlate the solubility of DAP-4 in nine pure solvents. Meanwhile, the relative average deviation (RAD) and the root mean square deviation ($RMSD$) were used to evaluate the accuracy and applicability of the correlation results. The relevant parameters of two models, as well as RAD and $RMSD$ are summarized in Tables 1–2.

The relative deviation (δ , Table S1), relative average deviation (RAD), and root means square deviation ($RMSD$) are defined by Eq. (3), Eq. (4) and Eq. (5), respectively. The related data are seen in Table 1.

$$\delta = \frac{x_i - x_{cal}}{x_i} \quad (3)$$

Table 1 Parameters of Apelbalt model

solvents	A	B	C	r	RAD/10 ²	RMSD/10 ⁵
ethyl acetate	737.7746	-36688.169	-107.9089	0.9990	1.5198	0.0226
ethanol	226.6876	-13376.9345	-33.7226	0.9983	1.4422	0.0900
acetone	-179.7818	5758.4264	28.4656	0.9997	0.6102	0.0509
formic acid	418.4958	-21183.6373	-62.2278	0.9969	1.3950	1.3627
deionized water	448.73105	-24018.4136	-65.84943	0.9938	3.8644	5.0373
cyclohexane	787.5094	-40595.1831	-116.3806	0.9980	2.6472	0.0429
methanol	329.3216	-18124.8205	-48.7665	0.9927	3.1475	0.4957
acetonitrile	-19.78466	-1844.827	2.97589	0.9918	1.9926	0.3693
n-propanol	1359.37341	-66641.2202	-201.3618	0.9954	4.2330	0.1238

Note: A, B, and C are the parameters of Apelbalt model. r is the correlation coefficient. RAD is relative average deviation. RMSD is root means square deviation.

Table 2 Model parameters of λh equation for DAP-4 in different solvents

solvents	λ	h	r	RAD/10 ²	RMSD/10 ⁵
ethyl acetate	0.0037	908547.89	0.9898	6.7563	0.0150
ethanol	0.0064	462658.57	0.9955	2.7651	0.0849
acetone	0.0116	257360.25	0.9990	1.5245	0.0396
formic acid	0.0281	71160.77	0.9886	3.3924	37.1958
deionized water	0.6636	5564.43	0.9943	4.5371	101.8719
cyclohexane	0.0252	178157.04	0.9905	8.1881	0.0264
methanol	0.0202	150322.07	0.9867	4.4271	1.4465
acetonitrile	0.0157	173470.68	0.9972	1.9225	0.4106
n-propanol	0.0254	169833.71	0.9834	14.7538	0.0793

Note: λ and h represent the model parameters of the λh equation. r is the correlation coefficient. RAD is relative average deviation. RMSD is root means square deviation.

$$RAD = \frac{1}{n} \sum \frac{|x_i - x_{cal}|}{x_i} \quad (4)$$

$$RMSD = \left[\frac{\sum_{i=1}^n (x_i - x_{cal})^2}{n-1} \right]^{1/2} \quad (5)$$

where x_{cal} is the solubility coefficient value calculated by the fitted model, and n is the number of data points for experimental measurement of solubility coefficient.

2.2.1 Apelbalt model

The modified Apelbalt equation^[32-34] was used to investigate the relationship between mole fraction solubility and temperature in different solvents, and the fitting results are shown in Table 1. It can be seen that the calculated values are in good agreement with the experimental results. The correlation coefficients are range from 0.9918 to 0.9997, which indicates that the Apelbalt equation model can corre-

late solubility data well. From Table 1, the correlation coefficient (r) is close to 1, relative average deviation (RAD) is less than 4.2330×10^{-2} , and the root means square deviation (RMSD) is less than 5.0373×10^{-5} , indicating that the Apelbalt equation fits the solubility coefficient data of DAP-4 in the above solvents well.

$$\ln x_i = A + \frac{B}{T} + C \ln(T) \quad (6)$$

where x_i , T(K), A, B, and C are the solubility coefficient of DAP-4, temperature, and the model parameters determined by experimental solubility coefficient data, respectively.

2.2.2 λh model

The λh equation^[35-36] (see Eq.(7)) proposed by Buchowski according to the solid-liquid equilibrium theory is used to correlate and fit the experimental data:

$$\ln \left[1 + \lambda \left(\frac{1 - x_i}{x_i} \right) \right] = \lambda h \left(\frac{1}{T} - \frac{1}{T_m} \right) \quad (7)$$

where T_m is the melting point of DAP-4 (638.15 K)^[19], λ and h represent the model parameters of the λh equation, respectively. The λ value reflects the non-ideality of the solution system, and the h value represents the excess mixing enthalpy of the solution.

The model parameters, the correlation coefficient r, RAD and RMSD are shown in Table 2. It can be seen that the fitting coefficient of the λh equation is between 0.9834 and 0.9990, which is slightly worse than that of Apelbalt model. Therefore, the Apelbalt model can better fit the solubility data in this study than the λh model.

According to the above results, for nine pure solvents, the maximal *RAD* values of modified Apelblat model and λh model are 4.23% and 14.75%, respectively. And the maximal *RMSD* values of modified Apelblat model and λh model are 5.03×10^{-5} and 101.87×10^{-5} , respectively. For λh model, the solubility sequence of DAP-4 in nine pure solvents were approximately positively correlated with the λ values and approximately negatively correlated with the h values. The solubility increases with the increasing of temperature and tends to enlarge λ . The excessively high λ value also means that the solution tends to be non-ideal, which may lead to significant volume change and thermal effect during dissolution. Theoretically, the larger the mixing enthalpy (h), the greater the external energy required for solute dissolution, and the greater the energy barrier to be overcome. Therefore, it can be inferred that the smaller the mixing enthalpy, the easier the dissolution of DAP-4. The analysis results of thermodynamic models show that the experimental values of the solubility of DAP-4 are basically consistent with the calculated values, which is credible.

2.3 The dissolution thermodynamics of DAP-4

To better understand the dissolution process and dissolution behavior of DAP-4 in different solvents at different temperatures, the relationship between the logarithm of the solubility coefficient (x^j) and the temperature will be described by Van't Hoff equation based on the thermodynamic principle of solid-liquid equilibrium^[37], as shown in Eq.(8):

$$\ln(x_i) = a + \frac{b}{T} \quad (8)$$

where a and b are constant; the model parameters a , b , the correlation coefficient r obtained by fitting the Van't Hoff equation, relative average deviation (*RAD*), and the root mean square deviation (*RMSD*) value are calculated by eq.(4) and eq. (5) are shown in Table 3.

For an ideal solution system, the Van't Hoff equation^[37] can be used to know that the logarithmic value of the solubility coefficient has a linear relationship with the absolute temperature:

Table 3 Model parameters of Van't Hoff equation for DAP-4 in different solvents

solvents	a	b	r	<i>RAD</i> /10 ²	<i>RMSD</i> /10 ⁵
ethyl acetate	1.0107	-3777.9	0.9893	6.1437	0.0985
ethanol	0.0396	-3092.2	0.9973	2.2455	0.1641
acetone	0.0215	-2923.1	0.9986	1.5395	0.1489
formic acid	0.2654	-2205.3	0.9880	3.5922	4.0590
deionized water	6.16 00	-3935.6	0.9921	5.1396	7.3946
cyclohexane	5.3208	-5101.3	0.9922	6.9132	0.1410
methanol	1.5645	-3252	0.9924	1.9841	0.7904
acetonitrile	0.214	-2751.8	0.9978	4.2234	0.3919
<i>n</i> -propanol	6.0296	-5229.6	0.9787	12.7337	0.2611

Note: here a and b are the parameters of Van't Hoff equation. r is the correlation coefficient. *RAD* is relative average deviation. *RMSD* is root means square deviation.

$$\ln(x_i) = -\frac{\Delta H_d}{RT} + \frac{\Delta S_d}{R} \quad (9)$$

According to the Van't Hoff equation, $\ln x^j$ can find the slope of $1/T$:

$$\Delta G_d = \Delta H_d - T_{\text{mean}} \Delta S_d \quad (10)$$

$$T_{\text{mean}} = \frac{n}{\sum_{i=1}^n \frac{1}{T}} \quad (11)$$

where, ΔH_d represents the enthalpy change, $\text{kJ}\cdot\text{mol}^{-1}$; ΔS_d represents the entropy change, $\text{J}\cdot\text{k}^{-1}\cdot\text{mol}^{-1}$; ΔG_d represents the Gibbs free energy change, $\text{kJ}\cdot\text{mol}^{-1}$; R represents the gas constant; T_{mean} represents the average temperature, K, the value is 305.22 K; n represents the number of temperature points for determining solubility, respectively^[38-42].

The calculation results are shown in Table 4. The dissolution enthalpy changes of DAP-4 in the investigated solvents are all positive, indicating that all dissolution is endothermic. Meanwhile, $\Delta S_d > 0$, indicating that the dissolution process is entropy increasing process. What's more, the Gibbs free energies of DAP-4 dissolution process are all greater than 0, indicating that the dissolution processes are non-spontaneous. It can be seen from eq. (9) and Table 4 that the values of ΔG_d decrease with the increasing of temperature, indicating that higher temperature is beneficial to dissolution. Positive ΔH_d values were observed in tested solvents and the reason may be that there are strong interactions between

Table 4 Thermodynamic functions of DAP-4 in different solvents

solvents	ΔH_d / $\text{kJ}\cdot\text{mol}^{-1}$	ΔS_d / $\text{J}\cdot\text{K}^{-1}\cdot\text{mol}^{-1}$	ΔG_d / $\text{kJ}\cdot\text{mol}^{-1}$
ethyl acetate	31.41	8.4026	28.8448
ethanol	25.71	0.3292	25.6081
acetone	24.30	0.1788	24.2481
formic acid	18.33	2.2065	17.6614
deionized water	32.72	51.2141	17.0887
cyclohexane	42.41	44.2370	28.9100
methanol	27.04	13.0073	23.0667
acetonitrile	22.88	1.7842	22.3339
<i>n</i> -propanol	43.48	50.1299	28.1782

Note: T_{mean} is average temperature. ΔH_d is the enthalpy change. ΔS_d is the entropy change. ΔG_d is the enthalpy change.

DAP-4 and solvent molecules, while the newly formed bond energy between DAP-4 and solvent molecules are not enough to compensate for the energy required to break the original associative bonds of various solvents. The DAP-4 molecule contains various groups such as HClO_4 , NH_4^+ . Hence, the dissolution of DAP-4 in various tested solvents may cause different interactions such as dipole – dipole, hydrogen bonding^[43]. These interactions may be the reason that DAP-4 disrupts the alignment of solvent molecules and increases the entropy (ΔS_d). Furthermore, the solubility of DAP-4 is positive correlated with the values of ΔG_d in nine pure solvents.

3 Conclusion

In this work, the gravimetric method was used to study the dissolution behavior of DAP-4 in nine pure solvents at different temperatures (288–323 K). Furthermore, the dissolution model and the thermodynamic parameters of DAP-4 were obtained.

(1) The results shown that the solubility of DAP-4 in ethyl acetate, formic acid, absolute ethanol, acetone, and deionized water increases with the increasing of temperature and polarity. The solubility in water has the highest dependence on temperature and polarity, while the solubility in ethyl acetate has the lowest dependence on temperature and polarity. Therefore, deionized water can be con-

sidered as a suitable solvent for purification and recrystallization of DAP-4.

(2) The Apelbalt equation and the λh equation were used to establish the dissolution model of DAP-4. The results show that the Apelbalt model has a better fit than the λh model, which can better illustrate the dissolution behavior of DAP-4. In other word, the Apelbalt model can be used to predict the solubility data at other temperature in the system, which can provide a theoretical reference for the crystallization.

(3) In an ideal solution system, the Van't Hoff equation is used to calculate the thermodynamic function during the dissolution process. The results show that ΔH_d , ΔS_d and ΔG_d values of DAP-4 are all greater than zero, indicating that the dissolution is an endothermic, entropy increase and non-spontaneous process. Therefore, increasing the temperature is conducive to dissolution, which is consistent with the experimental data.

Declaration of Competing Interest: The authors declare that they have no known competing financial interests or personal relationships that could have appeared to influence the work reported in this paper.

References:

- [1] AGRAWAL J P. High energy materials: propellants, explosives and pyrotechnics[M]. New York: John Wiley & Sons, 2010.
- [2] KLAPÖTKO T M. High energy density materials[M]. Berlin: Springer, 2007.
- [3] MEYER R, KÖHLER J, HOMBURG A. Explosives[M]. New York: John Wiley & Sons, 2016.
- [4] FENG S, YIN P, HE C, PANG S, et al. Tunable dimroth rearrangement of versatile 1, 2, 3-triazoles towards high-performance energetic materials[J]. *Journal of Materials Chemistry A*, 2021, 9(20): 12291–12298.
- [5] TANG Y, HE C, IMLER G H, PARRISH D A, et al. AC—C bonded 5, 6-fused bicyclic energetic molecule: Exploring an advanced energetic compound with improved performance[J]. *Chemical Communications*, 2018, 54(75):10566–10569.
- [6] WANG Y, LIU Y, SONG S, et al. Accelerating the discovery of insensitive high-energy-density materials by a materials genome approach[J]. *Nature Communications*, 2018, 9(1): 2444.
- [7] YANG J, GONG X, MEI H, et al. Design of zero oxygen balance energetic materials on the basis of Diels-Alder chemistry[J]. *Journal of Organic Chemistry*, 2018, 83(23): 14698–14702.

- [8] YANG C, ZHANG C, ZHENG Z, et al. Synthesis and characterization of cyclo-pentazolate salts of NH_4^+ , NH_3OH^+ , N_2H_5^+ , $\text{C}(\text{NH}_2)_3^+$, and $\text{N}(\text{CH}_3)_4^+$ [J]. *Journal of the American Chemical Society*, 2018, 140(48): 16488–16494.
- [9] XU Y, WANG P, LIN Q, et al. Cationic and anionic energetic materials based on a new amphoteric[J]. *Science China Materials*, 2019, 62: 751–758.
- [10] WANG Q, SHAO Y, LU M. Amino-tetrazole functionalized fused triazolo-triazine and tetrazolo-triazine energetic materials [J]. *Chemical Communications*, 2019, 55(43): 6062–6065.
- [11] BELLAS M K, MATZGER A J. Achieving balanced energetics through cocrystallization[J]. *Angewandte Chemie International Edition*, 2019, 58(48): 17185–17188.
- [12] BENNION J C, SIDDIQI Z R, MATZGER A J. A melt castable energetic cocrystal[J]. *Chemical Communications*, 2017, 53(45): 6065–6068.
- [13] LANDENBERGER K B, BOLTON O, MATZGER A J. Energetic-energetic cocrystals of diacetone diperoxide (DADP): Dramatic and divergent sensitivity modifications via cocrystallization [J]. *Journal of the American Chemical Society*, 2015, 137(15): 5074–5079.
- [14] MA P, JIANG J C, ZHU S G. Synthesis, XRD and DFT studies of a novel cocrystal energetic perchlorate amine salt: Methylamine triethylenediamine triperchlorate [J]. *Combustion, Explosion and Shock Waves*, 2017, 53: 319–328.
- [15] BUSSHUYEV O S, BROWN P, MAITI A, et al. Ionic polymers as a new structural motif for high-energy-density materials [J]. *Journal of the American Chemical Society*, 2012, 134(3): 1422–1425.
- [16] GONG L, CHEN G, LIU Y, et al. Energetic metal-organic frameworks achieved from furazan and triazole ligands: Synthesis, crystal structure, thermal stability and energetic performance[J]. *New Journal of Chemistry*, 2021, 45(47): 22299–22305.
- [17] WU S, LI M, YANG Z, et al. Synthesis and characterization of a new energetic metal-organic framework for use in potential propellant compositions[J]. *Green Chemistry*, 2020, 22(15): 5050–5058.
- [18] CHEN S L, SHANG Y, HE C T, et al. Optimizing the oxygen balance by changing the A-site cations in molecular perovskite high-energetic materials[J]. *CrystEngComm*, 2018, 20(46): 7458–7463.
- [19] CHEN S L, YANG Z R, WANG B J, et al. Molecular perovskite high-energetic materials [J]. *Science China Materials*, 2018, 61: 1123–1128.
- [20] SHANG Y, YU Z H, HUANG R K, et al. Metal-free hexagonal perovskite high-energetic materials with $\text{NH}_3\text{OH}^+/\text{NH}_2\text{NH}_3^+$ as B-site cations[J]. *Engineering*, 2020, 6(9): 1013–1018.
- [21] ZHANG W X, CHEN S L, SHANG Y, et al. Molecular perovskites as a new platform for designing advanced multi-component energetic crystals [J]. *Energetic Materials Frontiers*, 2020, 1(3–4): 123–135.
- [22] SHANG Y, HUANG R K, CHEN S L, et al. Metal-free molecular perovskite high-energetic materials [J]. *Crystal Growth & Design*, 2020, 20(3): 1891–1897.
- [23] QI J A, PENG D, XI A, et al. Insight into the thermal decomposition properties of potassium perchlorate (KClO_4)-based molecular perovskite[J]. *Vacuum*, 2020, 175: 109257.
- [24] JIA Q, BAI X, ZHU S, et al. Fabrication and characterization of nano (H_2dabco) [$\text{K}(\text{ClO}_4)_3$] molecular perovskite by ball milling [J]. *Journal of Energetic Materials*, 2020, 38(4): 377–385.
- [25] LI X, HU S, CAO X, et al. Ammonium perchlorate-based molecular perovskite energetic materials: Preparation, characterization, and thermal catalysis performance with MoS_2 [J]. *Journal of Energetic Materials*, 2019, 38(2): 162–169.
- [26] DENG P, REN H, JIAO Q. Enhanced the combustion performances of ammonium perchlorate-based energetic molecular perovskite using functionalized graphene [J]. *Vacuum* 2019, 169: 108882.
- [27] DENG P, WANG H, YANG X, et al. Thermal decomposition and combustion performance of high-energy ammonium perchlorate-based molecular perovskite [J]. *Journal of Alloys and Compounds*, 2020, 827: 154257.
- [28] FANG H, GUO X, WANG W, et al. The thermal catalytic effects of CoFe-Layered double hydroxide derivative on the molecular perovskite energetic material (DAP-4) [J]. *Vacuum*, 2021, 193: 110503.
- [29] ZHAI P, SHI C, ZHAO S, et al. Thermal decomposition of ammonium perchlorate-based molecular perovskite from TG-DSC-FTIR-MS and ab initio molecular dynamics [J]. *RSC Advances*, 2021, 11(27): 16388–16395.
- [30] DENG P, REN H, JIAO Q. Enhanced thermal decomposition performance of sodium perchlorate by molecular assembly strategy [J]. *Ionics* 2020, 26: 1039–1044.
- [31] REN C, BAO Y, WANG Y, et al. Equilibrium solubility of p-nitroacetanilide in fifteen neat solvents: Determination, correlation, and solvent effect [J]. *Journal of Chemical & Engineering Data*, 2021, 67(1): 267–275.
- [32] ZHANG C, JIN S, CHEN S, et al. Solubilities of dihydroxylammonium 5, 5'-Bistetrazole-1, 1'-diolate in various pure solvents at temperatures between 293.15 and 323.15 K [J]. *Journal of Chemical & Engineering Data*, 2016, 61(5): 1873–1875.
- [33] APELBLAT A, MANZUROLA E. Solubilities of o-acetylsalicylic, 4-aminosalicylic, 3, 5-dinitrosalicylic, and p-toluic acid, and magnesium-DL-aspartate in water from T=(278 to 348) K [J]. *Journal of Chemical Thermodynamics*, 1999, 31(1): 85–91.
- [34] LIU J Q, CHEN S Y, JI B. Solubility and thermodynamic functions of isatin in pure solvents [J]. *Journal of Chemical & Engineering Data*, 2014, 59(11): 3407–3414.
- [35] KEHIAIAN H V. Group contribution methods for liquid mixtures: A critical review [J]. *Fluid Phase Equilibria*, 1983, 13: 243–252.
- [36] BUCHOWSKI H, KSIAZCZAK A, PIETRZYK S. Solvent activity along a saturation line and solubility of hydrogen-bonding solids [J]. *The Journal of Physical Chemistry*, 1980, 84(9): 975–979.
- [37] BENNEMA P, VAN EUPEN J, VAN DER WOLF B M, et al. Solubility of molecular crystals: Polymorphism in the light of solubility theory [J]. *International Journal of Pharmaceutics*, 2008, 351(1–2): 74–91.
- [38] ZHOU L, ZHANG P P, YANG G D, et al. Solubility of chrysin in ethanol and water mixtures [J]. *Journal of Chemical & Engineering Data*, 2014, 59(7): 2215–2220.

- [39] WANG N, FU Q, YANG G D, et al. Determination of the solubility, dissolution enthalpy and entropy of icariin in water, ethanol, and methanol[J]. *Fluid Phase Equilibria*, 2012, 324(324): 41-43.
- [40] LAN G C, WANG L, CHEN L Z, et al. Determination and correlation of the solubility of 3,4-bis(3-nitrofurazan-4-yl) furoxan (DNTF) in different solvents[J]. *Journal of Chemical Thermodynamics*, 2015, 89(5): 264-269.
- [41] KAIAZCZAK A, MOORTHI K, Nagata I, et al. Solid-solid transition and solubility of even n-alkanes[J]. *Fluid Phase Equilibria*, 1994, 95(389): 15-29.
- [42] ZHANG F, TANG Y, WANG L, et al. Solubility measurement and correlation for 2-naphthaldehyde in pure organic solvents and methanol + ethanol mixtures[J]. *Journal of Chemical & Engineering Data*, 2015, 60(8): 2502-2509.
- [43] WANG Z, PENG Y, CHENG X, et al. Investigation on Hansen solubility parameter, solvent effect and thermodynamic properties of 3-methylflavone-8-carboxylic acid dissolved in different solvents [J]. *Journal of Molecular Liquids*, 2022, 356: 119017.

分子钙钛矿含能材料 $(C_6N_2H_{14})(NH_4)(ClO_4)_3$ (DAP-4)在288~323 K下的各种溶剂中的溶解度

袁明羽¹, 刘强强¹, 尚宇², 周维¹, 邹俐¹, 高海翔³, 刘应乐¹

(1. 四川轻化工大学化学与环境工程学院, 四川 自贡 643000; 2. 西安近代化学研究所, 陕西 西安 710065; 3. 中国农业大学应用化学系, 北京 100193)

摘要: 溶解度是分子钙钛矿含能材料 $(H_6N_2H_{14})(NH_4)(ClO_4)_3$ (DAP-4)结晶工艺中的重要参数。本工作采用重量法研究了不同温度(288~323 K)下, DAP-4在不同溶剂(乙醇、乙酸乙酯、甲酸、去离子水、丙酮、环己烷、甲醇、乙腈、正丙醇)中的溶解行为, 并通过Apelblat方程和 λh 方程建立了溶解模型。基于固液平衡的热力学原理, 利用Van't Hoff方程得到了溶出热力学参数(ΔH_d , ΔS_d , ΔG_d)。结果表明, DAP-4在水中的溶解度最大, 在乙酸乙酯中的溶解度最小, 其值在不同溶剂中的溶解度随温度的增加而增加; Apelblat方程拟合的溶解模型优于 λh 方程拟合的结果; 热力学参数 ΔH_d , ΔS_d 和 ΔG_d 的均为正值说明DAP-4的溶解属于非自发吸热的过程。

关键词: 溶解度; 重量法; 分子钙钛矿含能材料; 溶解热力学参数

中图分类号: TJ55; O62

文献标志码: A

DOI: 10.11943/CJEM2022284

(责编: 王馨逸)